SUPPLEMENTARY FIGURE LEGENDS

Figure S1. Immunoblot analysis of yeast strain Y7092 expressing *P. syringae* T3SEs. Yeast strains expressing the FLAG-tagged T3SEs under the *GAL1* promoter were induced with 2% galactose for 7 to 8 hours. Whole cell extracts were prepared and total proteins were precipitated with trichloracetic acid. The protein pellets were resuspended in sample buffer and the samples were separated by 12% SDS-PAGE, followed by Western transfer. The expression of T3SEs was detected by mouse anti-FLAG primary antibodies, followed by goat anti-mouse secondary antibodies conjugated to horseradish peroxidase. The expected molecular weight of each T3SE is indicated in parentheses. A number of T3SEs (including AvrE, HopM1, HopAA1-1) that caused severe growth inhibition in yeast were not detected by immunoblot, presumably due to yeast cell death. Asterisks denote the expected T3SE bands.

Figure S2. Spot dilution assays to determine growth inhibition profiles of yeast expressing *P. syringae* T3SEs. The growth inhibition of yeast strain Y7092 expressing *P. syringae* T3SEs was characterized by plating serial dilutions of saturated yeast cultures on rich media containing glucose, galactose, glucose with 1 M sorbitol, galactose with 1 M sorbitol, glucose with 1 M NaCl and galactose with 1M NaCl. Each effector expressed by Y7092 is shown on the left of the figure, with the *P. syringae* pathovars indicated in parentheses. *ES* is *PmaES4326*, *DC* is *PtoDC3000*, *B728a* is *PsyB728a*, *Pph6* is *Pph1448a*, *Pav* is *PavBPIC631*, and *Pae* is *PaeNcPpB368*.

Figure S3. Extracted ion chromatograms, reversed phase chromatography and MS/MS spectra supporting identification of two distinct (singly) acetylated forms of the doubly charged HINKEL peptide, VFGPESLTENVYEDGVK. (**A, F**) Extracted ion chromatograms of tryptic peptides from the immunoprecipitated lysates of yeast cells co-expressing HINKEL with wild-type HopZ1a (**A**), or with the catalytic mutant, HopZ1a^{C216A} (**F**). Differences in retention time (RT) under reversed phase chromatography support post-translational modification (PTM) assignment since the peptides from HopZ1a-expressing cells (**A**) elute later (RT 45.50 min and RT 48.54 min) than the corresponding peptide from cells expressing HopZ1a^{C216A} (RT 43.29 min) (**F**). (**B, D, G**) Reversed phase chromatography of material from the peaks indicated in panels **A** and **F** allows identification of ions with mass/charge ratios matching theoretical predictions for the unmodified peptide VFGPESLTENVYEDGVK (**G**) or its acetylated variants (**B**, **D**). (**C, E, H**) Peptide fragmentation and analysis of the resulting MS/MS spectra allows identification of specific acetylation sites based on a nominal mass increase of 42 Da in subsets of the b- and y-ion series. Specifically, for the acetylated peptide species shown in panel **B**, the b6 ion shifts from *m*/*z* = 617.29 to *m*/*z* = 659.30, and the corresponding y-ion (y12) shifts from *m*/*z* = 1353.65 to 1395.66 (**C**, **H**). Similarly, for the second acetylated peptide species shown in panel **D**, the b8 ion shifts from *m*/*z* = 831.42 to 873.43 and the corresponding y-ion (y10) shifts from *m*/*z* = 1153.54 to 1195.54 (**E**, **H**). Thus, two distinct acetylated variants of the same peptide sequence were present in the sample with wild-type HopZ1a - VFGPE[S-

Ac]LTENVYEDGVK (**B**, **C**) and VFGPESL[T-Ac]ENVYEDGVK (**D**, **E**) - while only the unmodified peptide was detected in the presence of HopZ1a^{C216A} (**G**, **H**).

Figure S4. Extracted ion chromatograms, reversed phase chromatography and MS/MS spectra supporting acetylation of the doubly and triply charged MKRP1 peptide, EISCLQEELTQLR. (**A, D**) Extracted ion chromatograms of tryptic peptides from IP lysates of yeast cells co-expressing MKRP1 with wild-type HopZ1a (**A**), or the catalytic mutant, HopZ1a^{C216A} (**D**). (**B, E**) Reversed phase chromatography of material from the peaks with retention times of 43.59 (**A**), or 42.83 (**D**) allows identification of ions with mass/charge ratios matching theoretical predictions for doubly charged variants of the unmodified peptide, EISCLQEELTQLR (**E**), or of an acetylated variant (**B**). (**C, F**) Peptide fragmentation and analysis of the resulting MS/MS spectra allows identification of a specific acetylation site at T425 based on a nominal mass increases of 42 Da (acetylation) or of 24 Da (acetylation followed by loss of water/dehydration; 42-18 = 24 Da) in subsets of the b- and y-ion series. Specifically, for the acetylated peptide species shown in panel B, the b10 ion shifts from *m*/*z* = 1203.47 to a dehydrated b10(-H_2O) ion with *m*/*z* = 1227.50 (+24 Da) and the corresponding y-ion (y4) shifts from *m*/*z* = 517.43 to 559.46 (+42 Da) (**C**, **F**).

Figure S5. Extracted ion chromatograms, reversed phase chromatography and MS/MS spectra supporting acetylation of the doubly and triply charged MKRP1 peptide, EIYNETALNSQALEIENLK. (**A, D**) Extracted ion chromatograms of tryptic peptides from IP lysates of yeast cells co-expressing MKRP1 with wild-type HopZ1a

(**A**), or with the catalytic mutant, HopZ1a^{C216A} (**D**). (**B, E**) Reversed phase chromatography of material from the peaks with retention times of 50.43 (**A**) or 45.07 (**D**) allowed identification of ions with mass/charge ratios matching theoretical predictions for doubly charged variants of the unmodified peptide, EIYNETALNSQALEIENLK (**E**), or of an acetylated variant (**B**). (**C, F**) Peptide fragmentation and analysis of the resulting MS/MS spectra allows identification of the specific acetylation of T820 based on mass shifts of 42 Da in overlapping subsets of the ion series. The smallest b-ion showing the characteristic 42 Da mass shift was b6 (*m*/*z* = 750.33 to *m*/*z* = 792.34), while the corresponding y-ion, y14 was also the smallest to be shifted (*m*/*z* = 1543.87 to 1585.83) indicating acetylation of T820 (**F**, **C**).

Figure S6. Extracted ion chromatograms, reversed phase chromatography and MS/MS spectra supporting acetylation of the doubly and triply charged HopZ1a peptide, ELLDDETPSNTQFSASIDGFR. (**A, F**) Representative chromatograms of tryptic peptides from IP lysates of yeast cells co-expressing HopZ1a with either of the two kinesins, HINKEL and MKRP1. (**B, D, G**) Reversed phase chromatography of material from the peaks with retention times of 44.99 (**F**), 47.44 (**A**), and 48.87 (**A**) allowed identification of ions with mass/charge ratios matching theoretical predictions for the unmodified peptide, ELLDDETPSNTQFSASIDGFR, (**G**) or its acetylated variants (**B**, **D**). (**C, E, H**) Peptide fragmentation and analysis of the resulting MS/MS spectra allows identification of both singly- and doubly-acetylated variants of the HopZ1a peptide with sequence ELLDDETPSNTQFSASIDGFR. Specifically, acetylation of S346 (in the case of the acetylated peptide species shown in panel B) is inferred based on a

nominal mass increase of 42 Da for the b9 ion (shifts from *m*/*z* = 1000.44 to *m*/*z* = 1042.45) and for the corresponding y-ion (y13; shifts from *m*/*z* = 1429.67 to 1471.68) (**C**, **H**). Similarly, concurrent acetylation of both T342 and T348 (in the case of the acetylated peptide species shown in panel **D**) is inferred based on a nominal mass increase of 84 Da (two acetylated residues) 42 Da (one acetylated residue), or 24 Da (acetylation followed by loss of water/dehydration; 42-18 = 24 Da) in subsets of the b- and y-ion series. Specifically, the b7 ion shifts from *m*/*z* = 816.36 to b7-H2O *m*/*z* = 840.37 (+24 Da), while the corresponding y-ion (y15) shifts from *m*/*z* = 1627.77 to 1711.79 (+84 Da); these shifts identify acetylation of T342 but also indicate acetylation at a second site. In support of this assessment, b11 was also shifted by 84 Da (*m*/*z* = 1215.53 to *m*/*z* = 1299.55), while the corresponding y-ion, y11, was shifted by 42 Da (*m*/*z* = 1228.59 to 1270.60), indicating acetylation of T348 (**E**, **H**). These data thus indicate the presence of three acetylation sites present in two distinct acetylated variants of the same HopZ1a peptide sequence – ELLDDETP[S-Ac]NTQFSASIDGFR (**B**, **C**) and ELLDDE[T-Ac]PSN[T-Ac]QFSASIDGFR (**D**, **E**). Only the unmodified peptide was detected from the catalytic mutant, HopZ1a^{C216A} (**G**, **H**).

Figure S7. Zoomed-in views of the extracted ion chromatograms presented in Figure S7 (A and F). Enlarged figure to show that the peaks with retention times or 47.44 and 48.87 are present for HopZ1a^{wt} (**A**) but absent for the catalytic mutant, HopZ1a^{C216A} (**B**).

Figure S8. Acetylated HINKEL residues are proximal to the kinesin ATP-binding site. Acetylated HINKEL residues were mapped to a structure of human kinesin CENP-E (PDB 1T5C; (Garcia-Saez et al. 2004) and their side-chains are highlighted in red. Also shown is the bound ligand (ADP) and structural features that contribute to its binding site - R12, R14, P15, K92, T93, Y94, a Mg^{2+} ion (pink), and three water molecules (cyan).

Table S1. Confirmed synthetic genetic interactors and suppressors of HopZ1a HopZ1a.

TableS2. Confirmed synthetic genetic interactors and suppressors of HopF2.

TableS3. Confirmed synthetic genetic interactors of HopX1.

TableS4. Congruence scores for yeast genes with genetic interaction profiles similar to that of HopZ1a.

TableS5. Congruence scores for yeast genes with genetic interaction profiles similar to that of HopF2.

TableS6. Congruence scores for yeast genes with genetic interaction profiles similar to that of HopX1.

Supplementary Reference

Garcia-Saez, I., T. Yen, R. H. Wade, and F. Kozielski. 2004. "Crystal structure of the motor domain of the human kinetochore protein CENP-E." *J Mol Biol* 340 (5):1107-16. doi: 10.1016/j.jmb.2004.05.053.

Supplemental File Descriptions (to accompany file uploads to FigShare)

TableS1.xlsx lists confirmed synthetic genetic interactors and suppressors of HopZ1a

TableS2.xlsx lists confirmed synthetic genetic interactors and suppressors of HopF2

TableS3.xlsx lists confirmed synthetic genetic interactors of HopX1

TableS4.xlsx lists congruence scores for yeast genes with genetic interaction profiles similar to that of HopZ1a.

TableS5.xlsx lists congruence scores for yeast genes with genetic interaction profiles similar to that of HopF2.

TableS6.xlsx lists congruence scores for yeast genes with genetic interaction profiles similar to that of HopX1.

FigureS1.pdf shows immunoblot analysis of yeast strain Y7092 expressing *P. syringae* T3SEs.

FigureS2.pdf shows spot dilution assays to determine growth inhibition profiles of yeast expressing *P. syringae* T3SEs.

FigureS3.pdf shows extracted ion chromatograms, reversed phase chromatography and MS/MS spectra supporting identification of two distinct (singly) acetylated forms of the doubly charged HINKEL peptide, VFGPESLTENVYEDGVK.

FigureS4.pdf shows extracted ion chromatograms, reversed phase chromatography and MS/MS spectra supporting acetylation of the doubly and triply charged MKRP1 peptide, EISCLQEELTQLR.

FigureS5.pdf shows extracted ion chromatograms, reversed phase chromatography and MS/MS spectra supporting acetylation of the doubly and triply charged MKRP1 peptide, EIYNETALNSQALEIENLK.

FigureS6.pdf shows extracted ion chromatograms, reversed phase chromatography and MS/MS spectra supporting acetylation of the doubly and triply charged HopZ1a peptide, ELLDDETPSNTQFSASIDGFR.

FigureS7.pdf shows zoomed-in views of the extracted ion chromatograms presented in Figure S6.

FigureS8.pdf shows that acetylated HINKEL residues are proximal to the kinesin ATP-binding site.

FileS1.tar contains mass spectrometry raw data files from co-expression of HINKEL and MKRP1 with HopZ1a (HINKEL_HopZ1a_wt.raw, HINKEL_HopZ1a_CA.raw, MKRP1_HopZ1a_wt.raw, MKRP1_HopZ1a_CA.raw).

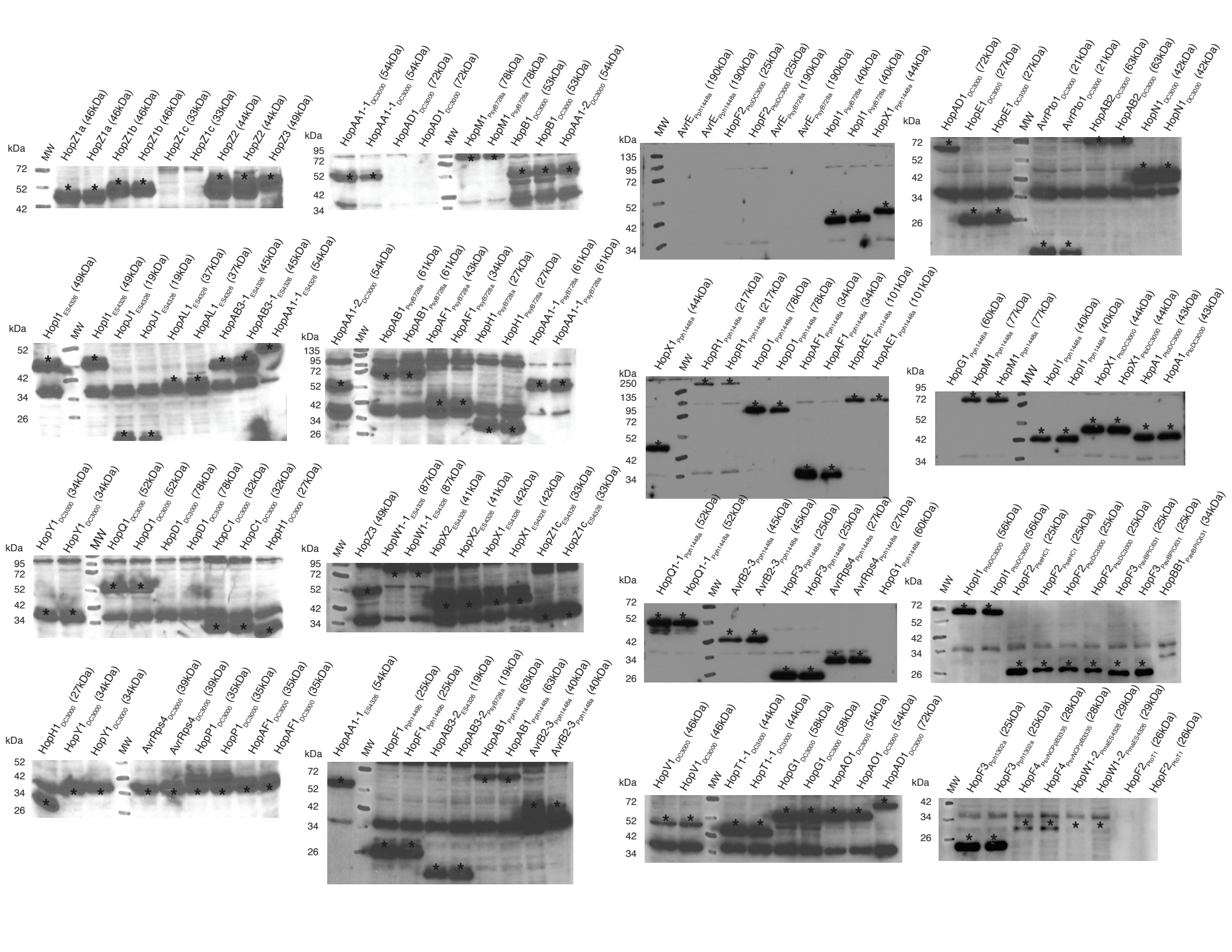
kDa
MW
HopZ1a (46kDa)
HopZ1a (46kDa)
HopZ1b (46kDa)
HopZ1b (46kDa)
HopZ1c (33kDa)
HopZ1c (33kDa)
HopZ2 (44kDa)
HopZ2 (44kDa)
HopZ3 (49kDa)
72
52
42
HopAA1-1DC3000 (54kDa)
HopAA1-1DC3000 (54kDa)
HopAD1DC3000 (72kDa)
HopAD1DC3000 (72kDa)
MW
HopM1Psyb728a (78kDa)
HopM1Psyb728a (78kDa)
HopB1DC3000 (53kDa)
HopB1DC3000 (53kDa)
HopAA1-2DC3000 (54kDa)
95
72
52
42
34
AvrEPph1448a (190kDa)
AvrEPph1448a (190kDa)
HopF2PtoDC3000 (25kDa)
HopF2PtoDC3000 (25kDa)
AvrEPsyb728a (190kDa)
AvrEPsyb728a (190kDa)
HopI1Psyb728a (40kDa)
HopI1Psyb728a (40kDa)
HopX1Pph1448a (44kDa)
135
95
72
52
42
34
HopAD1DC3000 (72kDa)
HopE1DC3000 (27kDa)
HopE1DC3000 (27kDa)
AvrPto1DC3000 (21kDa)
AvrPto1DC3000 (21kDa)
HopAB2DC3000 (63kDa)
HopAB2DC3000 (63kDa)
HopN1DC3000 (42kDa)
HopN1DC3000 (42kDa)
26
HopI1ES4326 (49kDa)
HopI1ES4326 (49kDa)
HopJ1ES4326 (19kDa)
HopJ1ES4326 (19kDa)
HopAL1ES4326 (37kDa)
HopAL1ES4326 (37kDa)
HopAB3-1ES4326 (45kDa)
HopAB3-1ES4326 (45kDa)
HopAA1-1ES4326 (54kDa)
HopAA1-2DC3000 (54kDa)
HopAB1Psyb728a (61kDa)
HopAB1Psyb728a (61kDa)
HopAF1Psyb728a (43kDa)
HopAF1Psyb728a (34kDa)
HopH1Psyb728a (27kDa)
HopH1Psyb728a (27kDa)
HopAA1-1Psyb728a (61kDa)
HopAA1-1Psyb728a (61kDa)
HopX1Pph1448a (44kDa)
HopR1Pph1448a (217kDa)
HopR1Pph1448a (217kDa)
HopD1Pph1448a (78kDa)
HopD1Pph1448a (78kDa)
HopAF1Pph1448a (34kDa)
HopAF1Pph1448a (34kDa)
HopAE1Pph1448a (101kDa)
HopAE1Pph1448a (101kDa)
250
HopG1Pph1448a (60kDa)
HopM1Pph1448a (77kDa)
HopM1Pph1448a (77kDa)
HopI1Pph1448a (40kDa)
HopI1Pph1448a (40kDa)
HopX1PtoDC3000 (44kDa)
HopX1PtoDC3000 (44kDa)
HopA1PtoDC3000 (43kDa)
HopA1PtoDC3000 (43kDa)
HopY1DC3000 (34kDa)
HopY1DC3000 (34kDa)
HopQ1DC3000 (52kDa)
HopQ1DC3000 (52kDa)
HopD1DC3000 (78kDa)
HopD1DC3000 (78kDa)
HopC1DC3000 (32kDa)
HopC1DC3000 (32kDa)
HopH1DC3000 (27kDa)
HopZ3 (49kDa)
HopW1-1ES4326 (87kDa)
HopW1-1ES4326 (87kDa)
HopX2ES4326 (41kDa)
HopX2ES4326 (41kDa)
HopX1ES4326 (42kDa)
HopX1ES4326 (42kDa)
HopZ1cES4326 (33kDa)
HopZ1cES4326 (33kDa)
HopQ1-1Pph1448a (52kDa)
HopQ1-1Pph1448a (52kDa)
AvrB2-3Pph1448a (45kDa)
AvrB2-3Pph1448a (45kDa)
HopF3Pph1448a (25kDa)
HopF3Pph1448a (25kDa)
AvrRps4Pph1448a (27kDa)
AvrRps4Pph1448a (27kDa)
HopG1Pph1448a (60kDa)
HopI1PtoDC3000 (56kDa)
HopI1PtoDC3000 (56kDa)
HopF2PseHC1 (25kDa)
HopF2PseHC1 (25kDa)
HopF2PtoDC3000 (25kDa)
HopF2PtoDC3000 (25kDa)
HopF3PseB728CS1 (25kDa)
HopF3PseB728CS1 (25kDa)
HopBB1PseB728CS1 (34kDa)
HopH1DC3000 (27kDa)
HopY1DC3000 (34kDa)
HopY1DC3000 (34kDa)
AvrRps4DC3000 (39kDa)
AvrRps4DC3000 (39kDa)
HopP1DC3000 (35kDa)
HopP1DC3000 (35kDa)
HopAF1DC3000 (35kDa)
HopAF1DC3000 (35kDa)
HopAA1-1ES4326 (54kDa)
HopF1Pph1448b (25kDa)
HopF1Pph1448b (25kDa)
HopAB3-2ES4326 (19kDa)
HopAB3-2Psyb728a (19kDa)
HopAB1Pph1448a (63kDa)
HopAB1Pph1448a (63kDa)
AvrB2-3Pph1448a (40kDa)
AvrB2-3Pph1448a (40kDa)
HopV1DC3000 (46kDa)
HopV1DC3000 (46kDa)
HopT1-1DC3000 (44kDa)
HopT1-1DC3000 (44kDa)
HopG1DC3000 (58kDa)
HopG1DC3000 (58kDa)
HopAO1DC3000 (54kDa)
HopAO1DC3000 (54kDa)
HopAD1DC3000 (72kDa)
HopF3Pph1302a (25kDa)
HopF3Pph1302a (25kDa)
HopF4PsyNCPPB3035 (28kDa)
HopF4PsyNCPPB3035 (28kDa)
HopW1-2PmaES4326 (29kDa)
HopW1-2PmaES4326 (29kDa)
HopF2PtoT1 (26kDa)
HopF2PtoT1 (26kDa)

Figure S1. Immunoblot analysis of yeast strain Y7092 expressing *P. syringae* T3SEs. Yeast strains expressing the FLAG-tagged T3SEs under the GAL1 promoter were induced with 2% galactose for 7 or 8 hours. Whole cell extracts were prepared and total proteins were precipitated with trichloracetic acid. The protein pellets were resuspended in sample buffer and the samples were separated by 12% SDS-PAGE, followed by Western transfer. The expression of T3SEs were detected by mouse anti-FLAG primary antibodies, followed by goat anti-mouse secondary antibodies conjugated to horseradish peroxidase. The expected molecular weight of each T3SEs is indicated in parentheses. A number of T3SEs (including AvrE, HopM1, HopAA-1) that caused severe growth inhibition in yeast were not detected by immunoblot, presumably due to yeast cell death. Asterisks denote the expected T3SE bands.

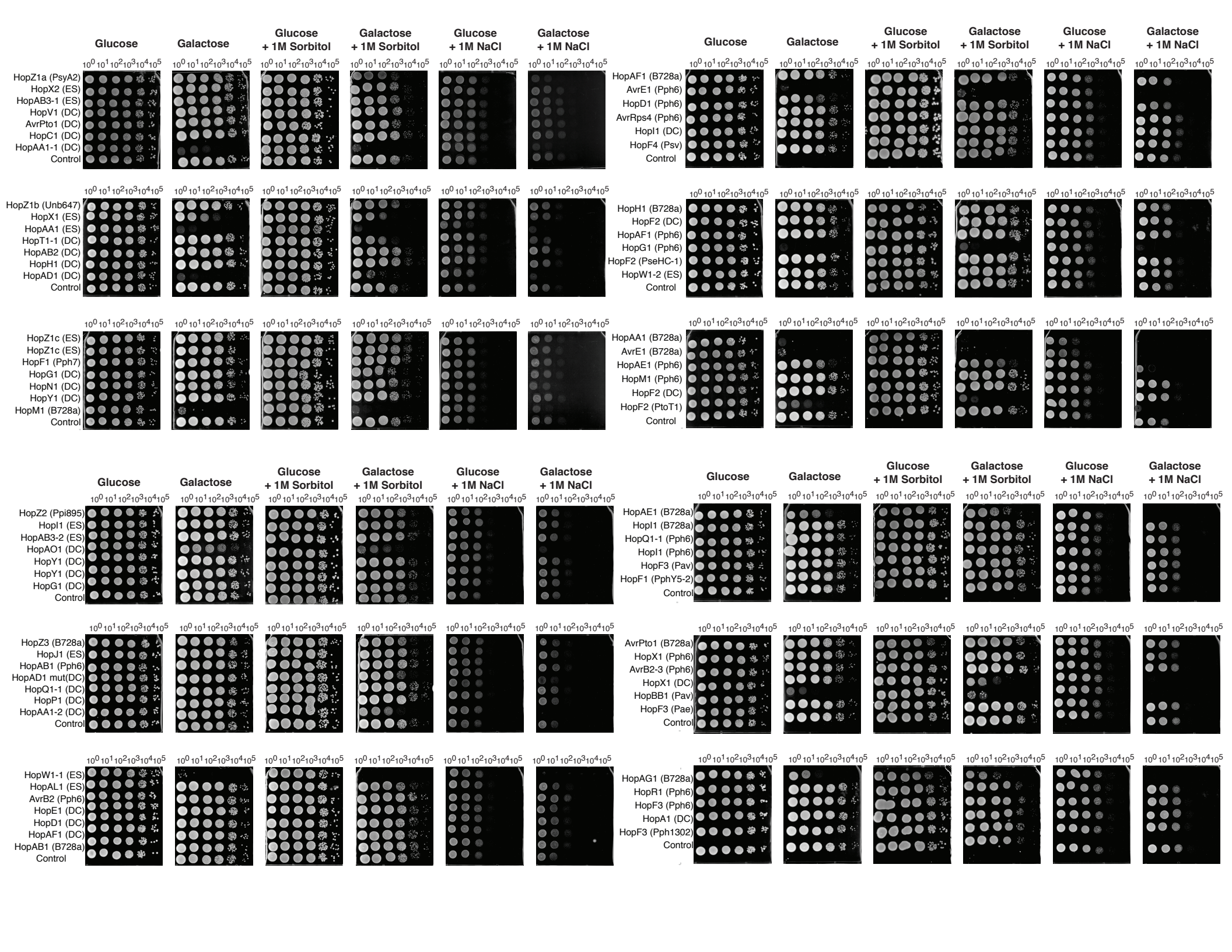
Glucose
Galactose
Glucose + 1M Sorbitol
Galactose + 1M Sorbitol
Glucose + 1M NaCl
Galactose + 1M NaCl
$10^0\,10^1\,10^2\,10^3\,10^4\,10^5$
HopZ1a (PsyA2)
HopX2 (ES)
HopAB3-1 (ES)
HopV1 (DC)
AvrPto1 (DC)
HopC1 (DC)
HopAA1-1 (DC)
Control
HopAF1 (B728a)
AvrE1 (Pph6)
HopD1 (Pph6)
AvrRps4 (Pph6)
HopI1 (DC)
HopF4 (Psv)
Control
HopZ1b (Unb647)
HopX1 (ES)
HopAA1 (ES)
HopT1-1 (DC)
HopAB2 (DC)
HopH1 (DC)
HopAD1 (DC)
Control
HopH1 (B728a)
HopF2 (DC)
HopAF1 (Pph6)
HopG1 (Pph6)
HopF2 (PseHC-1)
HopW1-2 (ES)
Control
HopZ1c (ES)
HopZ1c (ES)
HopF1 (Pph7)
HopG1 (DC)
HopN1 (DC)
HopY1 (DC)
HopM1 (B728a)
Control
HopAA1 (B728a)
AvrE1 (B728a)
HopAE1 (Pph6)
HopM1 (Pph6)
HopF2 (DC)
HopF2 (PtoT1)
Control
Glucose
Galactose
Glucose + 1M Sorbitol
Galactose + 1M Sorbitol
Glucose + 1M NaCl
Galactose + 1M NaCl
$10^0\,10^1\,10^2\,10^3\,10^4\,10^5$
HopZ2 (Ppi895)
HopI1 (ES)
HopAB3-2 (ES)
HopAO1 (DC)
HopY1 (DC)
HopY1 (DC)
HopG1 (DC)
Control
HopAE1 (B728a)
HopI1 (B728a)
HopQ1-1 (Pph6)
HopI1 (Pph6)
HopF3 (Pav)
HopF1 (PphY5-2)
Control
HopZ3 (B728a)
HopJ1 (ES)
HopAB1 (Pph6)
HopAD1 mut(DC)
HopQ1-1 (DC)
HopP1 (DC)
HopAA1-2 (DC)
Control
AvrPto1 (B728a)
HopX1 (Pph6)
AvrB2-3 (Pph6)
HopX1 (DC)
HopBB1 (Pav)
HopF3 (Pae)
Control
HopW1-1 (ES)
HopAL1 (ES)
AvrB2 (Pph6)
HopE1 (DC)
HopD1 (DC)
HopAF1 (DC)
HopAB1 (B728a)
Control
HopAG1 (B728a)
HopR1 (Pph6)
HopF3 (Pph6)
HopA1 (DC)
HopF3 (Pph1302)
Control

Figure S2. Spot dilution assays to determine growth inhibition profiles of yeast expressing *P. syringae* T3SEs. The growth inhibition of yeast strain Y7092 expressing *P. syringae* T3SEs was characterized by plating serial dilutions of saturated yeast cultures on rich media containing glucose, galactose, glucose with 1 M sorbitol, galactose with 1 M sorbitol, glucose with 1 M NaCl and galactose with 1M NaCl. Each effector expressed by Y7092 is shown on the left of the figure, with the *P. syringae* pathovars indicated in parentheses. *ES* is *PmaES4326*, *DC* is *PtoDC3000*, *B728a* is *PsyB728a*, *Pph6* is *Pph1448a*, *Pav* is *PavBPIC631*, and *Pae* is *PaeNcPpB368*.

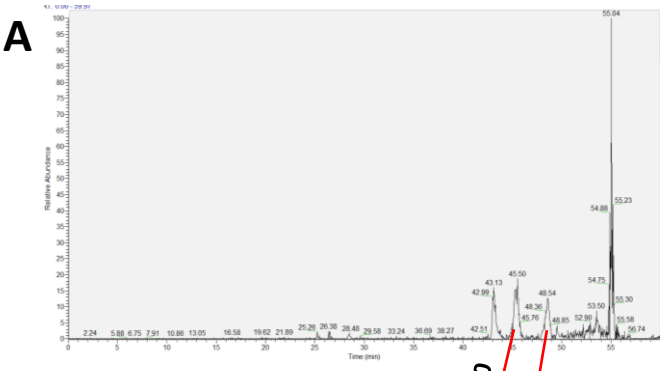

(A-E) Extracted ion chromatograms of the doubly charged HINKEL peptide VFGPESLTENVYEDGVK following co-expression with HopZ1a^{wt}

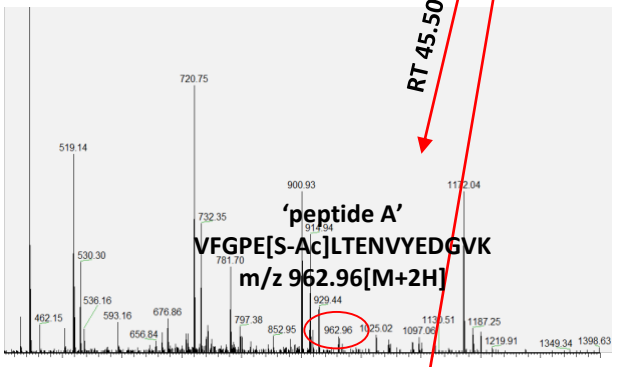

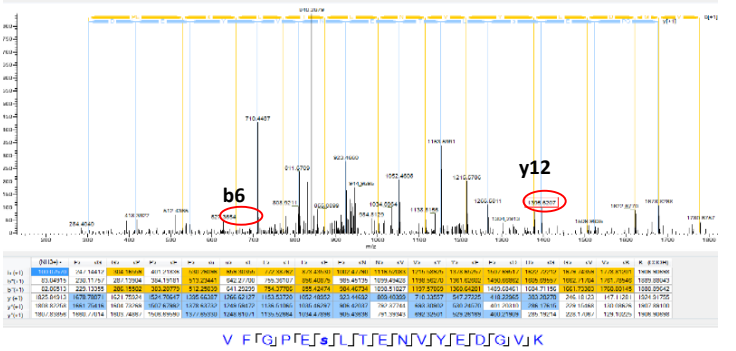

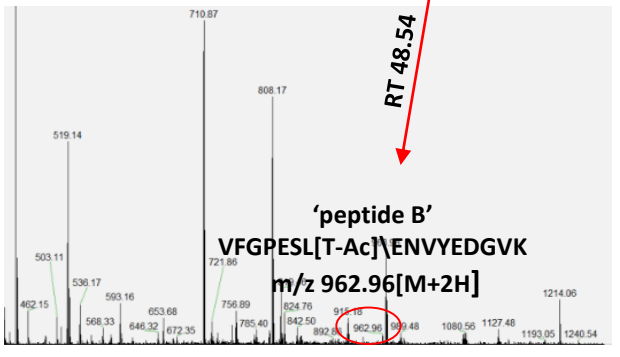

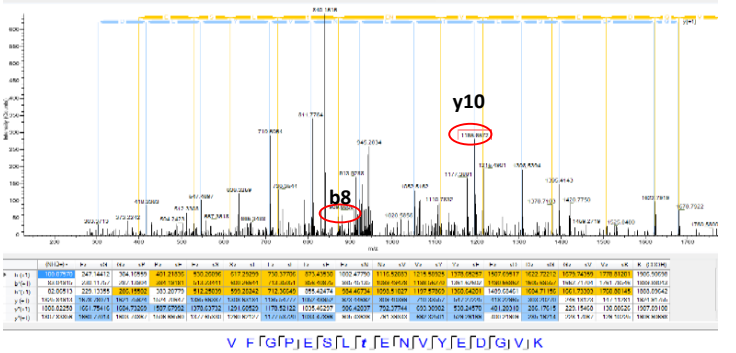

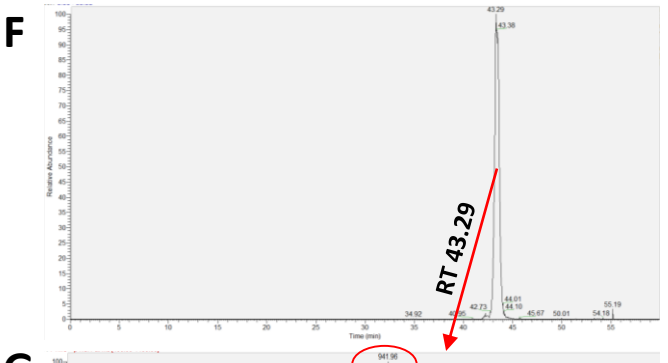

(F-H) Extracted ion chromatograms of the doubly charged HINKEL peptide VFGPESLTENVYEDGVK following co-expression with HopZ1a^{C216A}

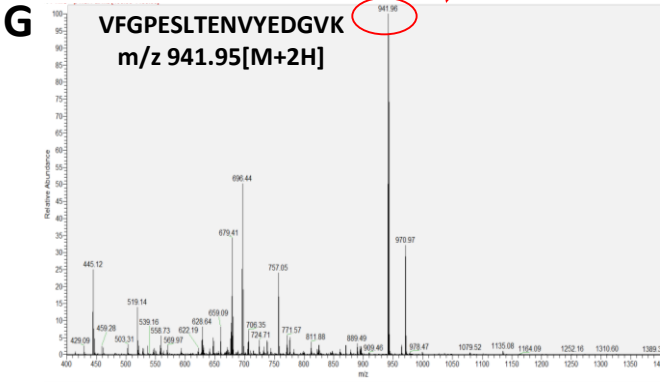

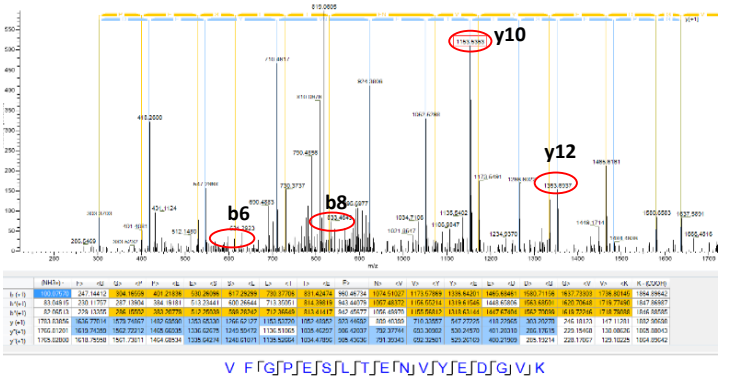

Figure S3. Extracted ion chromatograms, reversed phase chromatography and MS/MS spectra supporting identification of two distinct (singly) acetylated forms of the doubly charged HINKEL peptide, VFGPESLTENVYEDGVK. (A, F) Extracted ion chromatograms of tryptic peptides from the immunoprecipitated lysates of yeast cells co-expressing HINKEL with wild-type HopZ1a (A), or with the catalytic mutant, HopZ1a^{C216A} (F). Differences in retention time (RT) under reversed phase chromatography support post-translational modification (PTM) assignment since the peptides from HopZ1a-expressing cells (A) elute later (RT 45.50 min and RT 48.54 min) than the corresponding peptide from cells expressing HopZ1a^{C216A} (RT 43.29 min) (F). **(B, D, G)** Reversed phase chromatography of material from the peaks indicated in A and F allows identification of ions with mass/charge ratios matching theoretical predictions for the unmodified peptide VFGPESLTENVYEDGVK (G) or its acetylated variants (B, D). **(C, E, H)** Peptide fragmentation and analysis of the resulting MS/MS spectra allows identification of specific acetylation sites based on a nominal mass increase of 42 Da in subsets of the b- and y-ion series. Specifically, for the acetylated peptide species shown in panel B, the b6 ion shifts from m/z = 617.29 to m/z = 659.30, and the corresponding y-ion (y12) shifts from m/z = 1353.65 to 1395.66 (C, H). Similarly, for the second acetylated peptide species shown in panel D, the b8 ion shifts from m/z = 831.42 to 873.43 and the corresponding y-ion (y10) shifts from m/z = 1153.54 to 1195.54 (E, H). Thus, two distinct acetylated variants of the same peptide sequence were present in the sample with wild-type HopZ1a - VFGPE[S-Ac]LTENVYEDGVK (B, C) and VFGPESL[T-Ac]ENVYEDGVK (D, E) - while only the unmodified peptide was detected in the presence of HopZ1a^{C216A} (G, H).

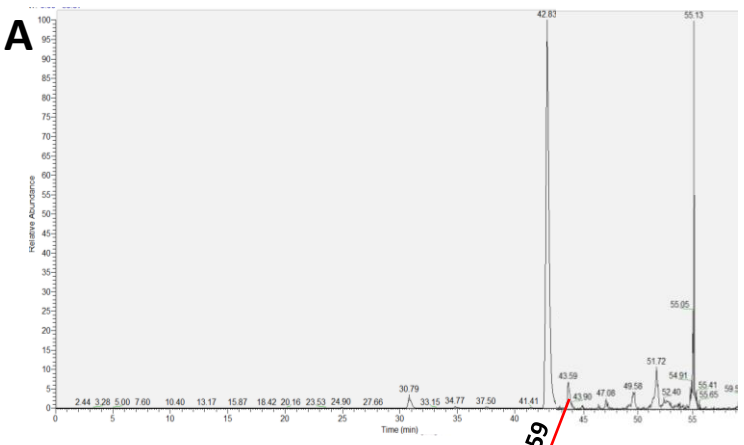

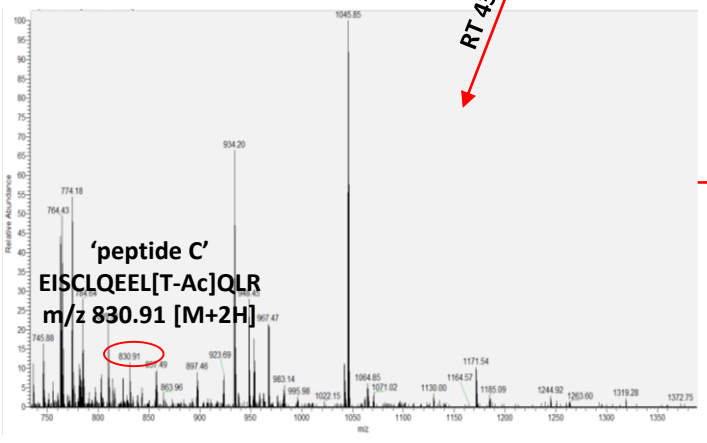

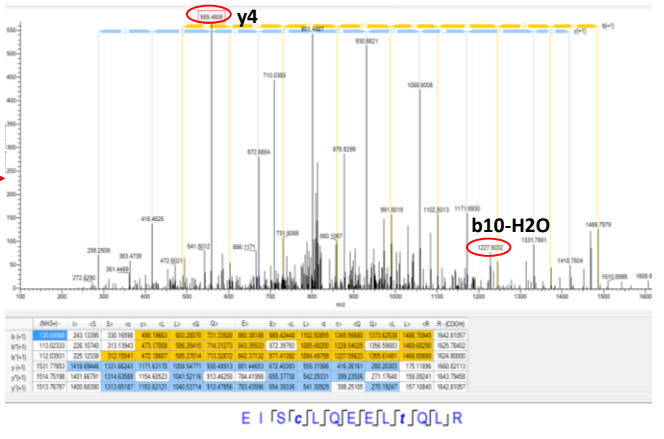

(A-C) Extracted ion chromatograms of the doubly charged MKRP1 peptide EISCLQEELTQLR following co-expression with HopZ1a^{wt}

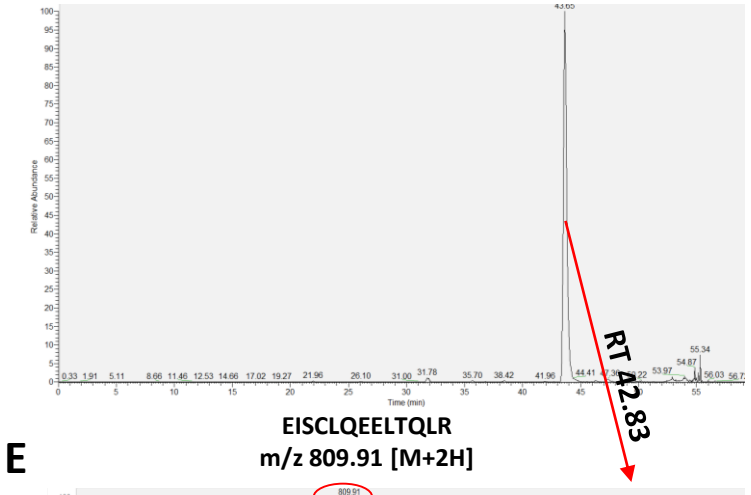

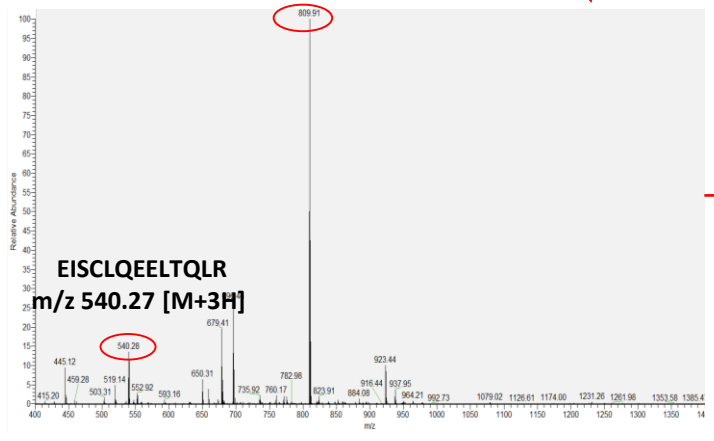

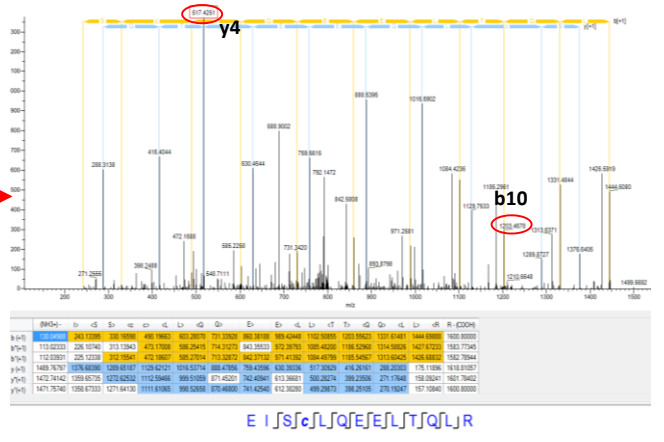

(D-F) Extracted ion chromatograms of the doubly charged MKRP1 peptide EISCLQEELTQLR following co-expression with HopZ1a^{C216A}

Figure S4 - **Extracted ion chromatograms, reversed phase chromatography and MS/MS spectra supporting acetylation of the doubly and triply charged MKRP1 peptide, EISCLQEELTQLR. (A, D)** Extracted ion chromatograms of tryptic peptides from IP lysates of yeast cells co-expressing MKRP1 with wild-type HopZ1a (A), or the catalytic mutant, HopZ1a^{C216A} (D). **(B, E)** Reversed phase chromatography of material from the peaks with retention times of 43.59 (A), or 42.83 (D) allows identification of ions with mass/charge ratios matching theoretical predictions for doubly charged variants of the unmodified peptide, EISCLQEELTQLR (E), or of an acetylated variant (B). **(C, F)** Peptide fragmentation and analysis of the resulting MS/MS spectra allows identification of a specific acetylation site at T425 based on a nominal mass increases of 42 Da (acetylation) or of 24 Da (acetylation followed by loss of water/dehydration; 42-18 = 24 Da) in subsets of the b- and y-ion series. Specifically, for the acetylated peptide species shown in panel B, the b10 ion shifts from *m*/*z* = 1203.47 to a dehydrated b10(-H_2O) ion with *m*/*z* = 1227.50 (+24 Da) and the corresponding y-ion (y4) shifts from *m*/*z* = 517.43 to 559.46 (+42 Da) (C, F).

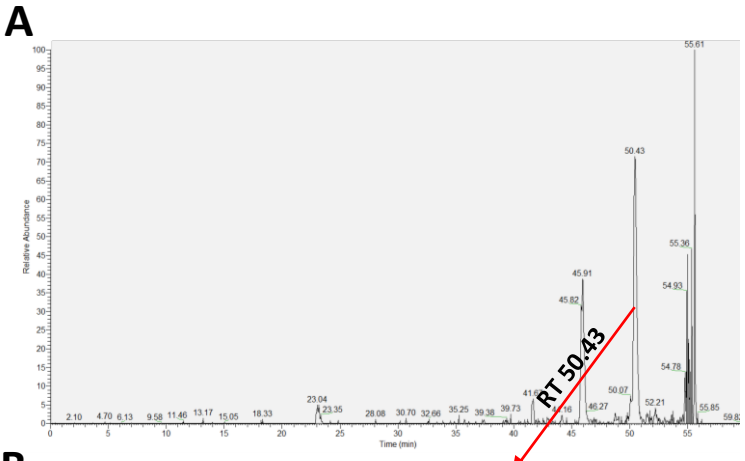

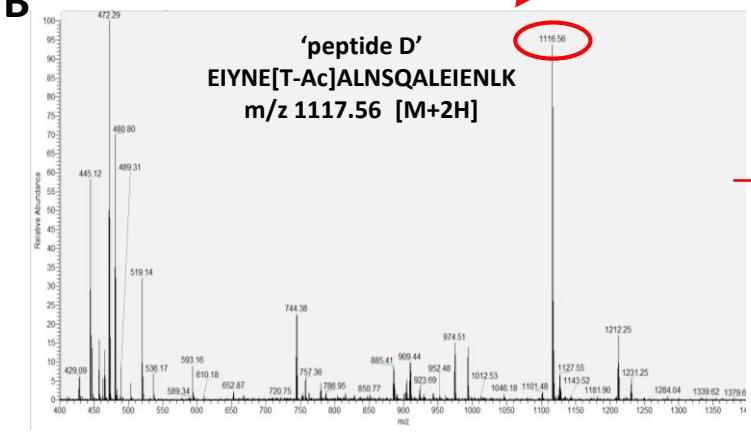

(A-C) Extracted ion chromatograms of the doubly charged MKRP1 peptide EIYNETALNSQALEIENLK following co-expression with HopZ1a^{wt}

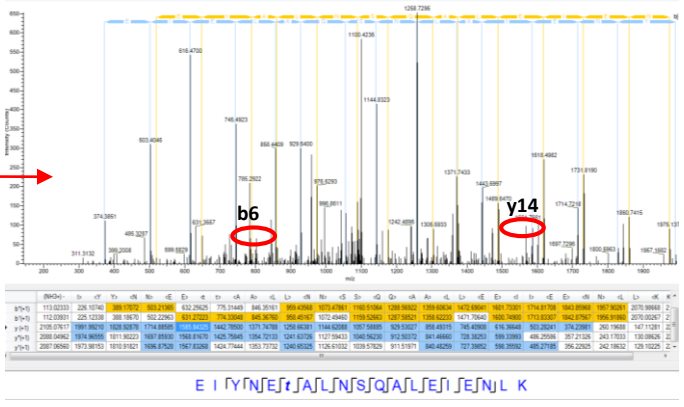

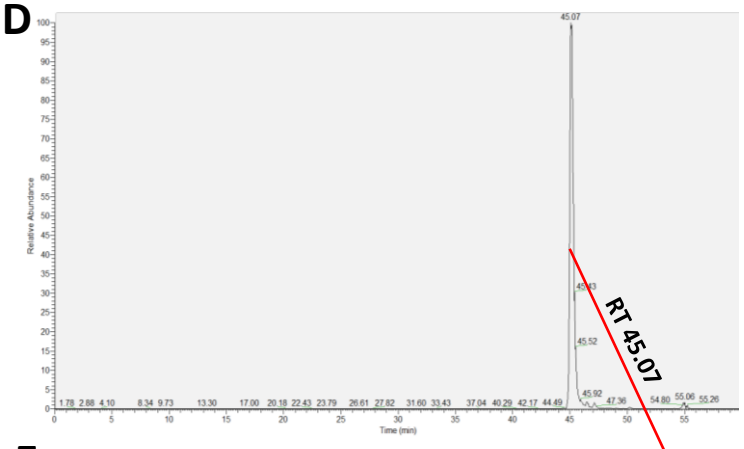

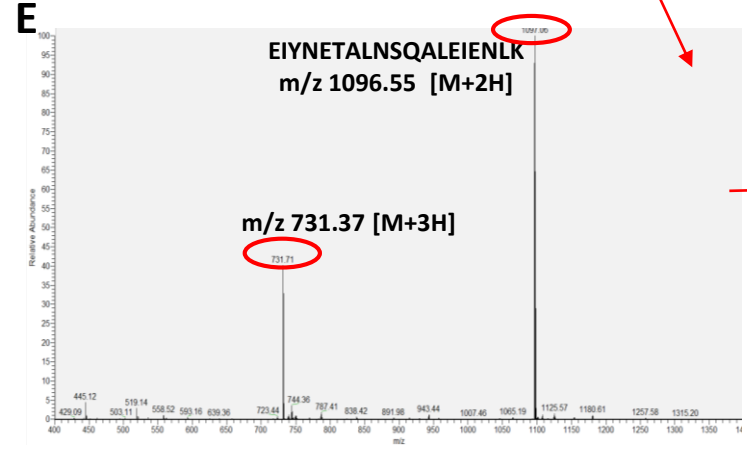

(D-F) Extracted ion chromatograms of the doubly charged MKRP1 peptide EIYNETALNSQALEIENLK following co-expression with HopZ1a^{C216A}

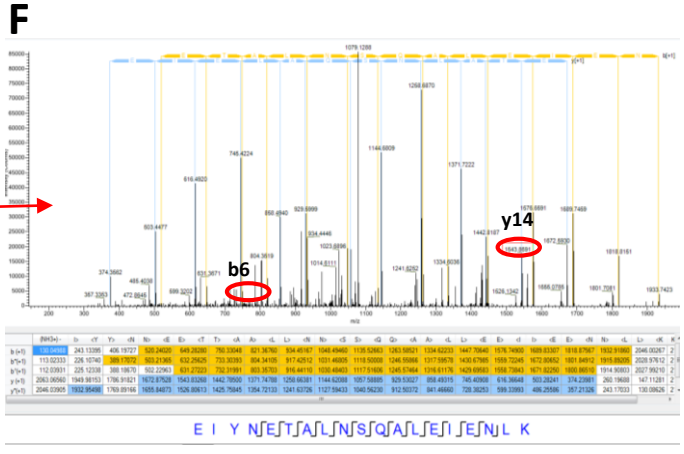

Figure S5 - **Extracted ion chromatograms, reversed phase chromatography and MS/MS spectra supporting acetylation of the doubly and triply charged MKRP1 peptide, EIYNETALNSQALEIENLK**. **(A, D)** Extracted ion chromatograms of tryptic peptides from IP lysates of yeast cells co-expressing MKRP1 with wild-type HopZ1a (A), or with the catalytic mutant, HopZ1a^{C216A} (D). **(B, E)** Reversed phase chromatography of material from the peaks with retention times of 50.43 (A) or 45.07 (D) allowed identification of ions with mass/charge ratios matching theoretical predictions for doubly charged variants of the unmodified peptide, EIYNETALNSQALEIENLK (E), or of an acetylated variant (B). **(C, F)** Peptide fragmentation and analysis of the resulting MS/MS spectra allows identification of the specific acetylation of T820 based on mass shifts of 42 Da in overlapping subsets of the ion series. The smallest b-ion showing the characteristic 42 Da mass shift was b6 (*m*/*z* = 750.33 to *m*/*z* = 792.34), while the corresponding y-ion, y14 was also the smallest to be shifted (*m*/*z* = 1543.87 to 1585.83) indicating acetylation of T820 (F, C).

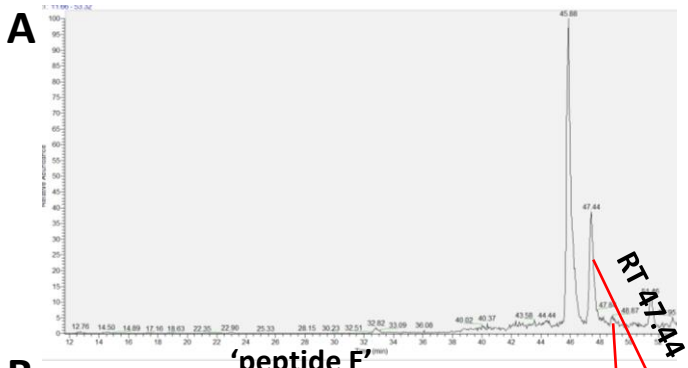

(A-E) Extracted ion chromatograms of the doubly and triply charged variants of peptide ELLDDETPSNTQFSASIDGFR from HopZ1a^{wt}

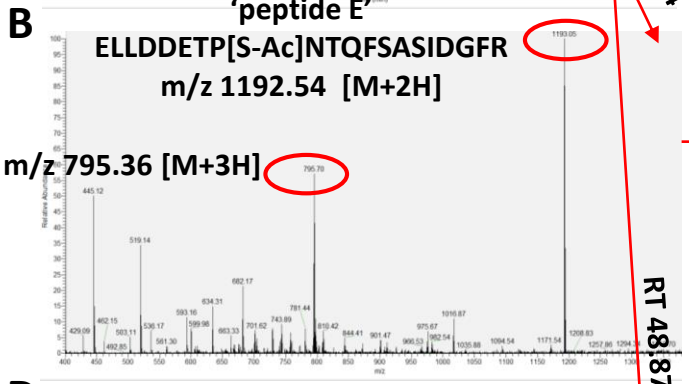

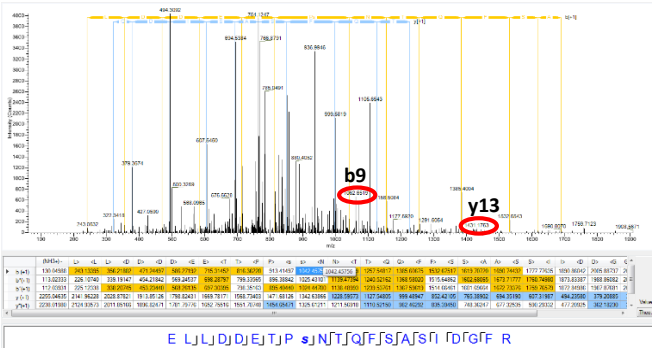

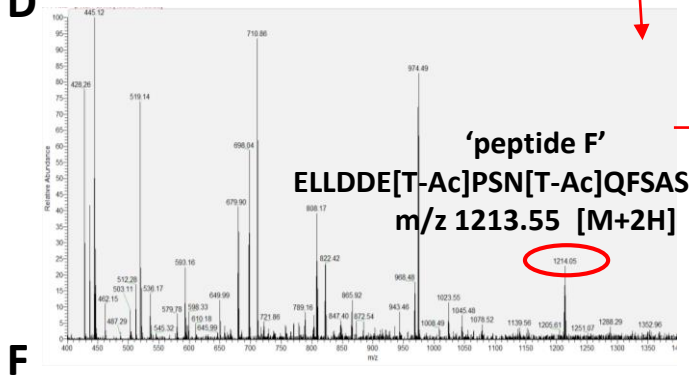

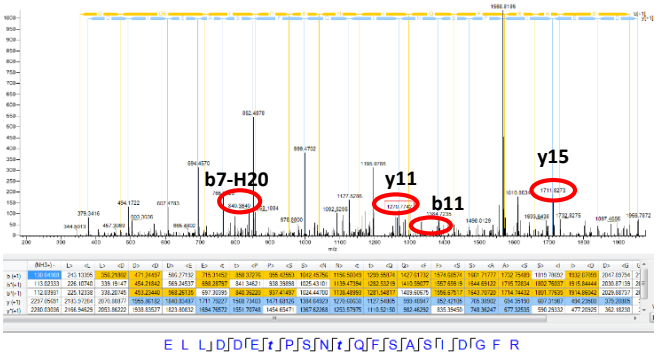

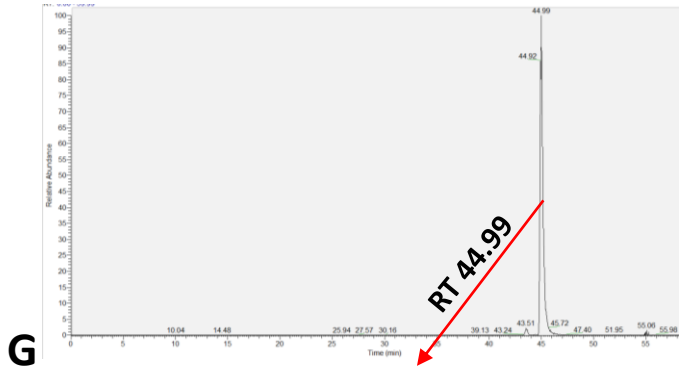

(F-H) Extracted ion chromatograms of the doubly and triply charged variants of peptide ELLDDETPSNTQFSASIDGFR from HopZ1a^{C216A}

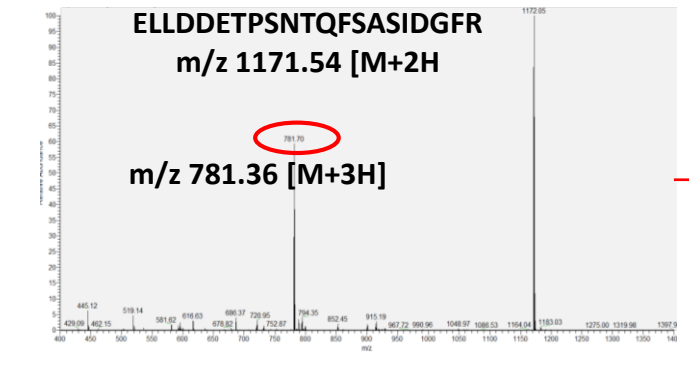

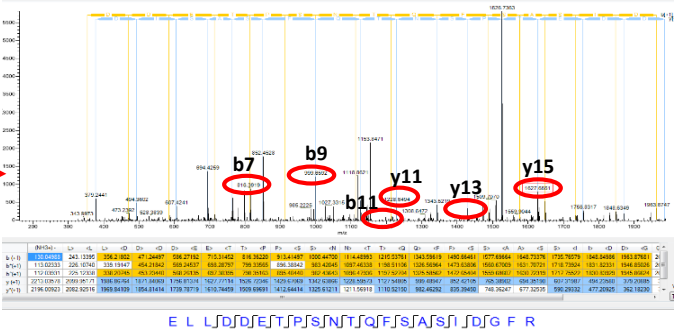

Figure S6 - Extracted ion chromatograms, reversed phase chromatography and MS/MS spectra supporting acetylation of the doubly and triply charged HopZ1a peptide, ELLDDETPSNTQFSASIDGFR. (A, F) Representative chromatograms of tryptic peptides from IP lysates of yeast cells co-expressing HopZ1a with either of the two kinesins, HINKEL and MKRP1. **(B, D, G)** Reversed phase chromatography of material from the peaks with retention times of 44.99 (F), 47.44 (A), and 48.87 (A) allowed identification of ions with mass/charge ratios matching theoretical predictions for the unmodified peptide, ELLDDETPSNTQFSASIDGFR, (G) or its acetylated variants (B, D). **(C, E, H).** Peptide fragmentation and analysis of the resulting MS/MS spectra allows identification of both singly- and doubly-acetylated variants of the HopZ1a peptide with sequence ELLDDETPSNTQFSASIDGFR. Specifically, acetylation of S346 (in the case of the acetylated peptide species shown in panel B) is inferred based on a nominal mass increase of 42 Da for the b9 ion (shifts from *m*/*z* = 1000.44 to *m*/*z* = 1042.45) and for the corresponding y-ion (y13; shifts from *m*/*z* = 1429.67 to 1471.68) (C, H). Similarly, concurrent acetylation of both T342 and T348 (in the case of the acetylated peptide species shown in panel D) is inferred based on a nominal mass increase of 84 Da (two acetylated residues) 42 Da (one acetylated residue), or 24 Da (acetylation followed by loss of water/dehydration; 42-18 = 24 Da) in subsets of the b- and y-ion series. Specifically, the b7 ion shifts from *m*/*z* = 816.36 to b7-H2O *m*/*z* = 840.37 (+24 Da), while the corresponding y-ion (y15) shifts from *m*/*z* = 1627.77 to 1711.79 (+84 Da); these shifts identify acetylation of T342 but also indicate acetylation at a second site. In support of this assessment, b11 was also shifted by 84 Da (*m*/*z* = 1215.53 to *m*/*z* = 1299.55), while the corresponding y-ion, y11, was shifted by 42 Da (*m*/*z* = 1228.59 to 1270.60), indicating acetylation of T348 (E, H). These data thus indicate the presence of three acetylation sites present in two distinct acetylated variants of the same HopZ1a peptide sequence – ELLDDETP[S-Ac]NTQFSASIDGFR (B, C) and ELLDDE[T-Ac]PSN[T-Ac]QFSASIDGFR (D, E). Only the unmodified peptide was detected from the catalytic mutant, HopZ1a^{C216A} (G,H).

A

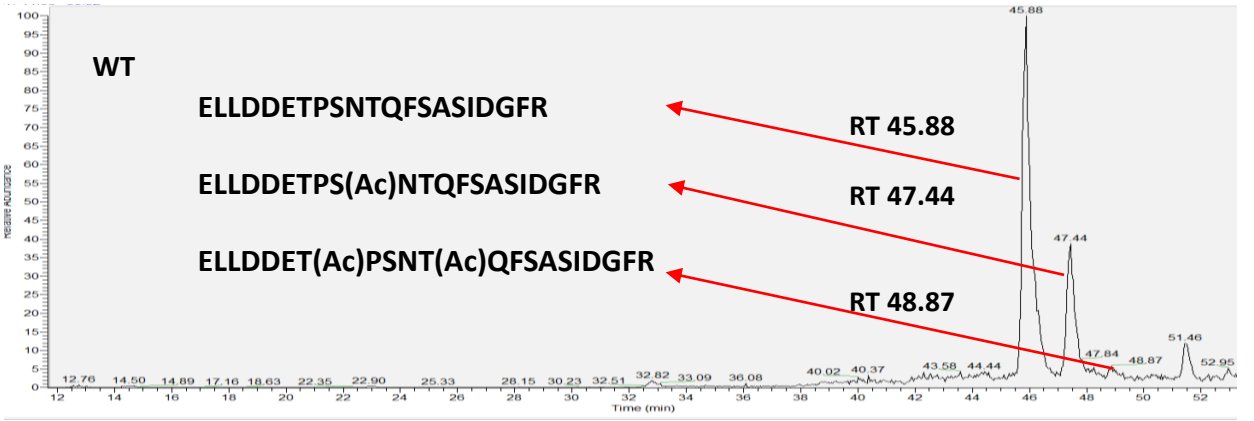

B

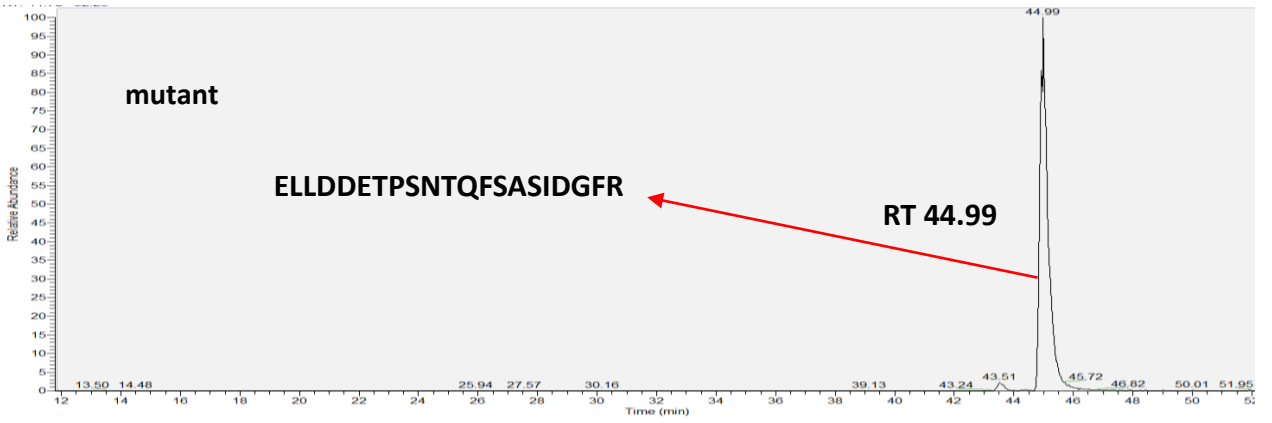

Figure S7 – Zoomed-in views of the extracted ion chromatograms presented in Figure S7 (A and F) more clearly demonstrate that the peaks with retention times or 47.44 and 48.87 are present for HopZ1a^{wt} (A) but absent for the catalytic mutant, HopZ1a^{C216A} (B).

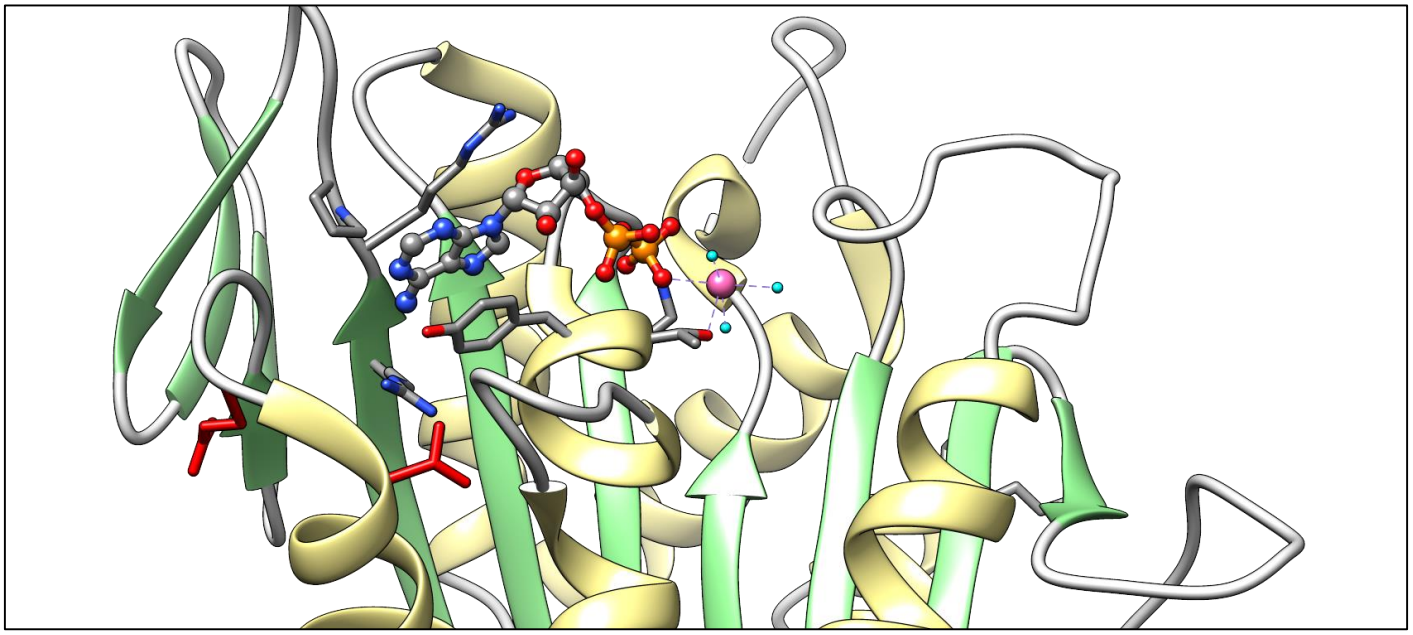

Figure S8 - Acetylated HINKEL residues are proximal to the kinesin ATP-binding site. Acetylated HINKEL residues were mapped to a structure of human kinesin CENP-E (PDB 1T5C; Garcia-Saez et al. 2004) by alignment of their kinesin motor domains using MUSCLE (Edgar, 2004). Sidechains of CENP-E residues (E57, T59) corresponding to acetylated HINKEL residues (S88, T90) are highlighted in red. Also shown is the bound ligand, ADP, and structural features that contribute to its binding site in CENP-E - R12, R14, P15, K92, T93, Y94, a Mg^{2+} ion (pink), and three water molecules (cyan).

Garcia-Saez, I., T. Yen, R. H. Wade, and F. Kozielski. 2004. "Crystal structure of the motor domain of the human kinetochore protein CENP-E." *J Mol Biol* 340 (5):1107-16. doi: 10.1016/j.jmb.2004.05.053.

Edgar, Robert C. 2004. "MUSCLE: Multiple Sequence Alignment with High Accuracy and High Throughput." *Nucleic Acids Research* 32 (5): 1792–97. https://doi.org/10.1093/nar/gkh340.